Inorganic Chemistry

Communication

pubs.acs.org/IC

Europium Pyrimidine-4,6-dicarboxylate Framework with a Single-Crystal-to-Single-Crystal Transition and a Reversible Dehydration/Rehydration Process

Hao-Ling Sun,*[,†] Dan-Dan Yin,[†] Qi Chen,[†] and Zhenqiang Wang*[,‡]

[†]Department of Chemistry and Beijing Key Laboratory of Energy Conversion and Storage Materials, Beijing Normal University, Beijing 100875, People's Republic of China

[‡]Department of Chemistry, The University of South Dakota, 414 E. Clark Street, Vermillion, South Dakota 57069, United States

Supporting Information

ABSTRACT: In this paper, a novel three-dimensional (3D) porous lanthanide−organic framework, $Eu_2(\mu_4\text{-pmdc})_2(OH)_2{\cdot}3H_2O$ (**1**), which is stable up to 400 °C, has been hydrothermally synthesized and characterized. It shows intriguing single-crystal-to-single-crystal transformation and reversible dehydration/rehydration phenomenon upon removal and rebinding of the lattice water molecules, which is supported by single-crystal X-ray diffraction, powder X-ray diffraction, and photoluminescence data.

In recent years, the research field on metal−organic frameworks (MOFs) has drawn increasing attention. Many researchers are focusing on the rational design and synthesis of MOFs with novel structures and potential applications such as gas separation and storage,[1] catalysis,[2] molecular magnetism,[3] and fluorescence.[4] Among various MOF-based materials, compounds with single-crystal-to-single-crystal (SCSC) transformations are particularly interesting because SCSC represents one of the most fascinating phenomena in chemistry and is attractive not only from a fundamental point of view but also in practical implications.[5−7] It offers a means to adjust or regulate the structures and properties of the materials through postsynthetic methods such as insertion/removal of the guest molecules,[5] modification of the organic ligands,[6] or changes in the coordination environment of the metal ions.[7] Among these strategies, insertion/removal of the guest molecules is most common.[5] The most appealing aspect of SCSC is that X-ray crystallographic analysis can provide sufficient and definite structural information on the phase change, which allows us to follow the progress of the transformation process. Thus, SCSC transformations open new routes to systematically studying the properties of the materials.[5−7] As a branch of MOFs, lanthanide−organic frameworks (LnOFs) show unusual structures and properties because of the unique feature of lanthanide ions with large radii, as well as their fascinating photoluminescent and magnetic behavior.[8−12] However, compared with the large number of examples of transition-metal-based MOFs with a SCSC transition, LnOFs with this phenomenon are much more rarely observed.[5g−j,6d,7b,c] Also removal of guests and/or coordination solvent molecules in a LnOF often results in an amorphous phase.[9] Herein, we report the synthesis, crystal structure, thermal gravimetric analysis (TGA), powder X-ray diffraction (PXRD), and photoluminescent properties of a porous LnOF, namely, $Eu_2(\mu_4\text{-pmdc})_2(OH)_2{\cdot}3H_2O$ (**1**; H_2pmdc = pyrimidine-4,6-dicarboxylic acid).

Needle crystals of **1** were obtained by a hydrothermal reaction (see the Supporting Information, SI). Single-crystal X-ray determination reveals that **1** contains a hydroxyl-bridging one-dimensional (1D) tape structure of $[Eu_2(\mu_3\text{-OH})_2]^{4+}$, which is further connected via $pmdc^{2-}$ ligands to result in a 3D coordination framework with 1D channels along the *a* axis (Figure 1). The asymmetric unit of **1** consists of two Eu^{3+} ions, two $pmdc^{2-}$ ligands, two μ_3-hydroxyl groups, and three lattice water molecules. The two crystallographically independent centers, Eu1 and Eu2, reside in similar coordination environments and are coordinated with seven oxygen atoms from four $pmdc^{2-}$ ligands, three hydroxyl groups, and one nitrogen atom

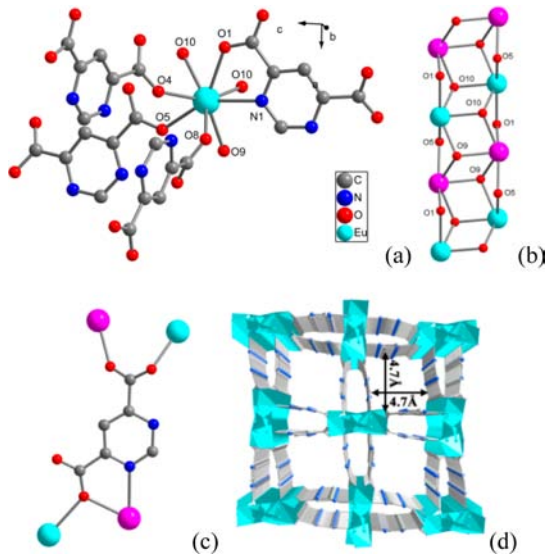

Figure 1. Coordination environment of Eu1 (a), a 1D tape structure constructed by a μ_3-hydroxyl (b), one type of bridging mode of $pmdc^{2-}$, (c) and the 3D porous structure with a 1D channel along the *a* axis (d) in **1**. The blue and purple spheres represent Eu1 and Eu2, respectively.

Received: November 21, 2012
Published: March 13, 2013

from the pyrimidine ring, resulting in a N1O7 donor set with a distorted square-antiprism coordination geometry (Figures 1a and S1a in the SI). Although the coordination environments in Eu1 and Eu2 are similar, orientation of the pyrimidine rings and carboxylate groups of $pmdc^{2-}$ and the bond lengths and angles around them are different (Figure S1 in the SI). The Eu−O distances are slightly shorter than the Eu−N distance, and these values are comparable to those found in the reported Eu^{3+} complexes (Table S2 in the SI).[9−12] The hydroxyl groups adopt a μ_3-bridging mode and connect three Eu^{3+} ions (O9 connects two Eu2 and one Eu1 ions, while O10 links two Eu1 and one Eu2 ions) with −O9−O9−O10−O10− alternations to produce a 1D tape structure along the *a* axis. The Eu···Eu distances are in the range of 3.829−3.989 Å, which is similar to those found in other lanthanide compounds with μ_3-hydroxyl bridges (Figure 1b).[9b,10] Both $pmdc^{2-}$ ligands in the asymmetric unit bridge two Eu1 and two Eu2 ions, adopting a μ_4-(κN,O,κO,κO′,κO′′) bridging mode (Figures 1c and S1b in the SI) and linking the 1D tape structures in an almost vertically arranged AB fashion. This results in a rather complicated 3D framework with 1D channels along the [001] direction (Figure 1d). Calculations based on the X-ray crystal structure show that the framework possesses a solvent-accessible volume of ca. 259 $Å^3$, corresponding to 13% of the unit cell.

In order to study the thermal stability of the 3D network of **1**, TGA was done and is shown in Figure S2 in the SI. **1** displays a first weight loss of 7.6% between room temperature and 110 °C, which is attributed to the release of three guest water molecules per formula unit and matches reasonably well with the calculated value (7.5%). There is no weight loss from 110 to 400 °C, which demonstrates that the dehydrated phase is thermally stable in this temperature range. Upon further heating, additional steps of weight loss in the range of 400−700 °C can be ascribed to decomposition of the framework. The remaining weight is 48.5%, indicating that Eu_2O_3 is the final product (calculated 48.5%).

To further probe the thermal stability and possible phase transition of the as-synthesized material, compound **1** was calcined at variable temperatures (Figure 2). The temperature-dependent PXRD patterns of **1** from room temperature to 400 °C indicate no changes and agree well with the simulated pattern based on the single-crystal X-ray diffraction data. The PXRD patterns together with the fact that the dehydration process occurs below 110 °C (according to the TGA curve) indicate that **1** may retain its crystalline structure even after losing its water molecules. The diffraction peaks have an obvious change when the temperature is increased to 500 °C. This is presumably due to decomposition of the framework. When further increases in the temperature, the sample becomes amorphous, as indicated by the broadness and disappearance of the diffraction peaks. Taken together, these results suggest that the framework structure of **1** is thermally stable up to 400 °C.

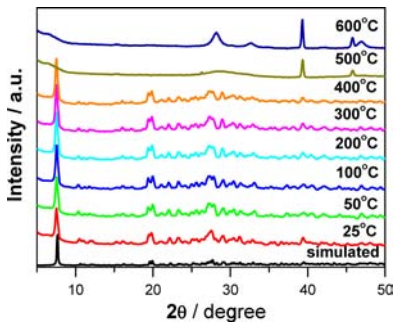

Figure 2. PXRD patterns of **1** at different temperatures along with the simulated pattern based on the single-crystal structure of the as-synthesized compound.

The above evidence suggests that it is possible to generate porous frameworks by removing the guest water molecules and compound **1** might be robust enough to undergo SCSC transitions rarely found in LnOFs. To test this hypothesis, the original sample was heated to 110 °C for 6 h under vacuum to obtain the dehydrated compound **2**. Indeed, **2** remained single crystalline, and we were able to successfully obtain its precise structural information by single-crystal X-ray diffraction. The cell parameters of **2** were almost identical with those of the parent compound, with a slight expansion of the unit cell (0.2%), suggesting that the porous structure is robust. The coordination environments around the Eu^{3+} ions and the bridging mode of $pmdc^{2-}$ ligands found in **2** are reminiscent of those found in **1** (Figure S3 in the SI). The dehydrated phase **2** has a similar solvent-accessible volume of ca. 261 $Å^3$, also corresponding to 13% of the unit cell. The TGA data of the dehydrated phase indicate that the water molecules are completely removed with nearly no weight loss below 110 °C, while the porous framework is also stable up to 400 °C (Figure S2 in the SI). Interestingly, when the dehydrated phase **2** was suspended in water at room temperature for 2 days, the sample regained its original weight and recovered the original structure, as indicated by a comparison of their PXRD patterns to that of the as-synthesized material (Figure S4 in the SI). Consequently, dehydration and rehydration are fully reversible, and the rehydrated sample retains the porous framework upon repeated dehydration.

The solid-state luminescent properties of **1** were studied upon the dehydration/rehydration processes. Both the dehydrated/rehydrated and original phases show emission spectra with characteristic emissions of Eu^{3+} (Figures 3 and S5 in the SI). The excitation spectrum monitored at 612 nm consists of a broad band and a few narrow bands. The broad band peaking around 278 nm is ascribed to the $\pi-\pi^*$ ligand transition, and the narrow bands are attributed to the intra-$4f^6$ electron transitions of Eu^{3+}.[11] The emission spectrum under 316 nm excitation shows five sharp emission peaks at 548, 593, 612, 653, and 696 nm, which are assigned to $^5D_0 \rightarrow {}^7F_J$ (J = 0−4) transitions of Eu^{3+} ions, respectively. The peaks at 548, 653, 593, and 696 nm attributed to the magnetic-dipole transitions are noticeably weaker than the electric-dipole-induced $^5D_0 \rightarrow$

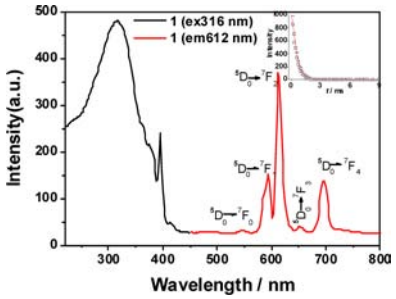

Figure 3. Solid-state excitation/emission spectra and the decay pattern (inset) of **1**.

dx.doi.org/10.1021/ic302556r | Inorg. Chem. 2013, 52, 3582−3584

$^7F_2$ transition at 612 nm, indicating that the coordination environment around Eu^{3+} ions is in low symmetry with the absence of inversion centers.[12] To better understand the luminescent properties of the original and dehydrated/rehydrated phases, the $^5D_0$ lifetime of the Eu^{3+} ion was monitored under excitation at 316 nm and the most intense emission at 612 nm ($^5D_0 \rightarrow {}^7F_2$). The room temperature lifetime value of **1** was determined to be 0.48 ms by monoexponentially fitting the emission decay pattern shown in the inset of Figure 3.

Interestingly, when the water molecules were removed to obtain the dehydrated sample **2**, its solid-state photoluminescent properties are evidently modified, with the lifetime increasing to 0.53 ms. This is likely due to the quenching effect of the luminescent state by high-frequency-vibrating water molecules and is in agreement with the finding published previously.[13] Furthermore, when the dehydrated sample was suspended in water to give rise to the rehydrated phase, its photoluminescent properties recover, with the lifetime changing back to 0.47 ms (0.48 ms for the original sample), further validating the reversibility of the dehydration/rehydration processes (Table S3 in the SI). In addition, the emission quantum yields (Φ_{QY}) were determined to be 8.9%, 11.0%, and 9.4% for the original, dehydrated, and rehydrated phases, respectively, which provides further evidence for a reversible dehydrated/rehydration process.[14]

In conclusion, a novel 3D porous LnOF stable up to 400 °C has been hydrothermally synthesized and thoroughly characterized. Upon removal and rebinding of the guest water molecules, it shows unusual SCSC transformation and reversible dehydration/rehydration phenomenon that is supported by single-crystal XRD, PXRD, and photoluminescence data. Furthermore, compared with the original sample **1**, the dehydrated phase **2** has modified photoluminescent behavior with a longer lifetime and higher emission quantum yield. These results suggest that our LnOF system represents a promising candidate for structural probing and fluoroimmunoassays.

■ ASSOCIATED CONTENT

Ⓢ Supporting Information

Details of the experimental section, crystal data and selected bond lengths, coordination environment of Eu2 and another bridging mode of $pmdc^{2-}$, TGA, PXRD, solid-state excitation/emission spectra and the decay pattern (inset) of dehydrated/rehydrated phases, and X-ray crystallographic data in CIF format of compounds **1** and **2** (CCDC 906997 and 906998). This material is available free of charge via the Internet at http://pubs.acs.org.

■ AUTHOR INFORMATION

Corresponding Author

*E-mail: haolingsun@bnu.edu.cn (H.-L.S), Zhenqiang.Wang@usd.edu (Z.W.).

Notes

The authors declare no competing financial interest.

■ ACKNOWLEDGMENTS

This work was supported by the National Natural Science Foundation of China (Grants 20801006 and 21171023). We thank Prof. Zhe-Ming Wang of Peking University for help with crystal structure refinement.

■ REFERENCES

(1) (a) Fernandez, C. A.; Liu, J.; Praveen, K. T.; Denis, M. S. *J. Am. Chem. Soc.* **2012**, *134*, 9046. (b) Zheng, S. T.; Wu, T.; Zhang, J. A.; Chow, M.; Nieto, R. A.; Feng, P. Y.; Bu, X. H. *Angew. Chem., Int. Ed.* **2010**, *49*, 5362.

(2) (a) Ma, L. Q.; Falkowski, J. M.; Abney, C.; Lin, W. *Nat. Chem.* **2010**, *2*, 838. (b) Song, F.; Wang, C.; Falkowski, J. M.; Ma, L.; Lin, W. *J. Am. Chem. Soc.* **2010**, *132*, 15390.

(3) (a) Moushi, E. E.; Stamatatos, T. C.; Wernsdorfer, W.; Nastopoulos, V.; Christou, G.; Tasiopoulos, A. J. *Angew. Chem., Int. Ed.* **2006**, *45*, 7722. (b) Dechambenoit, P.; Long, J. R. *Chem. Soc. Rev.* **2011**, *40*, 3249.

(4) (a) Allendorf, M. D.; Bauer, C. A.; Bhakta, R. K.; Houk, R. J. *Chem. Soc. Rev.* **2009**, *38*, 1330. (b) Jiang, H. L.; Tatsu, Y.; Lu, Z. H.; Xu, Q. *J. Am. Chem. Soc.* **2010**, *132*, 5586. (c) Wanderley, M. M.; Wang, C.; Wu, C. D.; Lin, W. *J. Am. Chem. Soc.* **2012**, *134*, 9050. (d) Rocha, J.; Carlos, L. D.; Paz, F. A.; Ananias, D. *Chem. Soc. Rev.* **2011**, *40*, 926.

(5) (a) Kawano, M.; Fujita, M. *Coord. Chem. Rev.* **2007**, *251*, 2592 and references cited therein. (b) Inokuma, Y.; Arai, T.; Fujita, M. *Nat. Chem.* **2010**, *2*, 780. (c) Su, Z.; Chen, M.; Okamura, T. A.; Chen, M. S.; Chen, S. S.; Sun, W. Y. *Inorg. Chem.* **2011**, *50*, 985. (d) Maji, T. K.; Mostafa, G.; Matsuda, R.; Kitagawa, S. *J. Am. Chem. Soc.* **2005**, *127*, 17152. (e) Yoshida, Y.; Inoue, K.; Kurmoo, M. *Inorg. Chem.* **2009**, *48*, 267. (f) Yoshida, Y.; Inoue, K.; Kurmoo, M. *Inorg. Chem.* **2009**, *48*, 10726. (g) Cai, Y. P.; Zhou, X. X.; Zhou, Z. Y.; Zhu, S. Z.; Thallapally, P. K.; Liu, J. *Inorg. Chem.* **2009**, *48*, 6341. (h) Gustafsson, M.; Bartoszewicz, A.; Martin-Matute, B.; Sun, J.; Grins, J.; Zhao, T.; Li, Z.; Zhu, G.; Zou, X. *Chem. Mater.* **2010**, *22*, 3316. (i) Gustafsson, M.; Su, J.; Yue, H.; Yao, Q.; Zou, X. *Cryst. Growth Des.* **2012**, *12*, 3243. (j) Lama, P.; Aijaz, A.; Neogi, S.; Barbour, L. J.; Bharadwaj, P. K. *Cryst. Growth Des.* **2010**, *10*, 3410.

(6) (a) Wang, Z.; Cohen, S. M. *Chem. Soc. Rev.* **2009**, *38*, 1315. (b) Liu, D.; Ren, Z. G.; Li, H. X.; Lang, J. P.; Li, N. Y.; Abrahams, B. F. *Angew. Chem., Int. Ed.* **2010**, *49*, 4767. (c) Ou, Y. C.; Zhi, D. S.; Liu, W. T.; Ni, Z. P.; Tong, M. L. *Chem.—Eur. J.* **2012**, *18*, 7357. (d) Michaelides, A.; Skoulika, S.; Siskos, M. G. *Chem. Commun.* **2011**, *47*, 7140.

(7) (a) Allan, P. K.; Xiao, B.; Teat, S. J.; Knight, J. W.; Morris, R. E. *J. Am. Chem. Soc.* **2010**, *132*, 3605. (b) Manos, M. J.; Kyprianidou, E. J.; Papaefstathiou, G. S.; Tasiopoulos, A. J. *Inorg. Chem.* **2012**, *51*, 6308. (c) Ghosh, S. K.; Zhang, J. P.; Kitagawa, S. *Angew. Chem., Int. Ed.* **2007**, *46*, 7965.

(8) (a) Li, M.; Liu, B.; Wang, B.; Wang, Z.; Gao, S.; Mohamedally, K. *Dalton Trans.* **2011**, *40*, 6038. (b) Bogani, L.; Sangregorio, C.; Sessoli, R.; Gatteschi, D. *Angew. Chem., Int. Ed.* **2005**, *44*, 5817. (c) Cepeda, J.; Balda, R.; Beobide, G.; Castillo, O.; Fernandez, J.; Luque, A.; Perez-Yanez, S.; Roman, P. *Inorg. Chem.* **2012**, *51*, 7875.

(9) (a) Zhu, W. H.; Wang, Z. M.; Gao, S. *Inorg. Chem.* **2007**, *46*, 1337. (b) Li, X.; Sun, H. L.; Wu, X. S.; Qiu, X.; Du, M. *Inorg. Chem.* **2010**, *49*, 1865.

(10) (a) Gandara, F.; Garcia-Cortes, A.; Cascales, C.; Gomez-Lor, B.; Gutierrez-Puebla, E.; Iglesias, M.; Monge, A.; Snejko, N. *Inorg. Chem.* **2007**, *46*, 3475. (b) Zhang, X. J.; Xing, Y. H.; Sun, Z.; Han, J.; Zhang, Y. H.; Ge, M. F.; Niu, S. Y. *Cryst. Growth Des.* **2007**, *7*, 2041.

(11) Girginova, P. I.; Paz, F. A. A.; Soares-Santos, P. C. R.; SaFerreira, R. A.; Carlos, L. D.; Amaral, V. S.; Klinowski, J.; Nogueira, H. I. S.; Trindade, T. *Eur. J. Inorg. Chem.* **2007**, 4238.

(12) (a) Kirby, A. F.; Foster, D.; Richardson, F. S. *Chem. Phys. Lett.* **1983**, *95*, 507. (b) Zhou, T. H.; Yi, F. Y.; Li, P. X.; Mao, J. G. *Inorg. Chem.* **2010**, *49*, 905.

(13) (a) Xia, J.; Zhao, B.; Wang, H. S.; Shi, W.; Ma, Y.; Song, H. B.; Cheng, P.; Liao, D. Z.; Yan, S. P. *Inorg. Chem.* **2007**, *46*, 3450. (b) Zhao, Y.; Jiao, C. Q.; Sun, Z. G.; Zhu, Y. Y.; Chen, K.; Wang, C. L.; Li, C.; Zheng, M. J.; Tian, H.; Sun, S. H.; Chu, W. *Cryst. Growth Des.* **2012**, *12*, 3191.

(14) Liu, T. F.; Zhang, W. J.; Sun, W. H.; Cao, R. *Inorg. Chem.* **2011**, *50*, 5242.